Original Article

Skin wound healing promoted by novel curcumin-loaded micelle hydrogel

Ping Zhou[1], Hao Zhou[2], Jian Shu[1], Shaozhi Fu[3], Zhu Yang[4]

[1]Department of Radiology, the Affiliated Hospital of Southwest Medical University, Luzhou, China; [2]Post Graduation Training Department, West China Hospital, Sichuan University, Chengdu, China; [3]Department of Oncology, the Affiliated Hospital of Southwest Medical University, Luzhou, China; [4]Nursing Department, People's Hospital of Luxian County, Luzhou, China

Contributions: (I) Conception and design: S Fu; (II) Administrative support: P Zhou; (III) Provision of study materials or patients: H Zhou; (IV) Collection and assembly of data: Z Yang; (V) Data analysis and interpretation: P Zhou; (VI) Manuscript writing: All authors; (VII) Final approval of manuscript: All authors.

Correspondence to: Ping Zhou. Department of Radiology, the Affiliated Hospital of Southwest Medical University, Luzhou 646000, China. Email: zhouping1@126.com.

Background: The development of biomaterials with the ability to promote skin wound healing is an important topic in the field of biomedical science. In this study, a topical curcumin (Cur) gel [Cur/hyaluronic acid (HA)] was prepared by combining curcumin-loaded PCL-b-PEG-b-PCL (PECE) nanomicelles (PCEC/Cur) and HA to effectively promote skin wound healing. Continuous drug release from PCEC/Cur can provide long-term protection and treatment of skin wounds.

Methods: The study was completed in two stages. The first stage (*in vitro*): PCEC/Cur were prepared by thin film hydration method. The second stage (*in vivo*): 36 anesthetized rats were used to prepare a round full-thickness skin defect wound with a diameter of 23 mm on the dorsal side of the spine, and the rats were randomly divided into 4 groups with 9 rats in each group.

Results: The results showed that wounds in the Cur/HA group were restored to normal after 14 days after operation, representing 96%±3% wound healing. Hematoxylin and eosin (HE) staining showed that hair follicles in the Cur/HA group were visible and that the re-epithelialization time was earlier. Masson staining showed that Cur/HA promoted the formation of collagen fibers. Immunohistochemical observation showed that angiogenesis and subsequent healing of the wound surface was enhanced in the Cur/HA group.

Conclusions: The injectable hyaluronic acid gel complex Cur/HA is a promising candidate material for a wound dressing to promote healing.

Keywords: Curcumin (Cur); nanomicelles; sodium hyaluronate; skin defect

Submitted May 04, 2021. Accepted for publication Jul 02, 2021.
doi: 10.21037/atm-21-2872
View this article at: https://dx.doi.org/10.21037/atm-21-2872

Introduction

The skin is the largest organ of the human body, accounting for 5–15% of the total body weight with an area of 1.5–2 m^2. The primary function of the skin is to protect internal body tissues from the outside environment by providing a protective barrier (1). Skin damage caused by trauma, burns, infections, tumors, and metabolic diseases is commonly seen in clinical practice. The primary treatment of skin defects is to close the wound as soon as possible, in order to reduce complications such as body consumption and microbial invasion (2).

Of the several therapeutic strategies available, covering the wound with a dressing to promote skin healing is the most commonly used In the clinical. At present, hydrocolloid dressings, alginate dressings, drug-carrying dressings, and hydrogel dressings are widely used in clinical practice (3). Antibiotic dressings can play a bactericidal role and promote wound healing, but they have the disadvantage

Figure 1 Chemical structure of curcumin.

of antibiotic resistance. Silver ion dressings are antibacterial, highly efficient, and long lasting, with the added advantage of not having drug resistance (4). However, silver ion dressings are expensive and can be toxic. Conversely, hydrogels consist of networks of hydrophilic polymers that are held together by physical or chemical bonds that absorb water (5). In recent years, research on hydrogels has received increased attention. Hydrogels are widely used in the medical field for drug delivery (6,7), tissue engineering, as sensors (8), and (6,9,10) in antibiotic therapy. With the development of tissue engineering techniques, new drugs have been added to the kit of traditional dressings in order to improve effective treatment (11).

In the clinical, cross-linked hydrophilic polymers retain water well and can be used either as a wound dressing or as a wound healing drug carrier. Hydrophilic polymers can absorb wound exudate, and the interconnected pores provide a three-dimensional network with large volume and surface area for drug binding (12). Hydrogels can be prepared from natural polymers or synthetic polymers, but they are typically derived from extracellular matrix (ECM). One of the main components of the ECM is hyaluronic acid (HA), which consists of disaccharide units of D-glucuronic acid-N-acetylglucosamine. Curcumin (Cur) is a substance extracted from the rhizome of the genus *Curcuma* of the family *Zingiberaceae*, which include phenols, terpenoids, and other compounds (10). Its chemical structure is shown in *Figure 1*. Cur has strong antioxidant, anti-inflammatory, and antibacterial properties (13,14) that promote healing of damaged skin (15). Recently, Cur has attracted attention as a local drug due to its extensive pharmacological properties, low toxicity, and good tolerance. However, due to its poor water solubility and low oral absorption bioavailability, its clinical application is limited (16). Cur has the effect of anti-scar formation, can induce apoptosis and reduce the secretion of inflammatory factors. Hydrogel carriers have obvious advantages in delivering drugs to the epidermis and dermis to increase drug concentration at the treatment site and reduce systemic adverse reactions. In order to circumvent these deficiencies, a hydrogel-based nanodrug delivery system for Cur has been developed.

The purpose of this study was to investigate the wound-healing effects of a topical Cur/HA composed of PCL-b-PEG-b-PCL (PECE) nanomicelles (PCEC/Cur) and HA. Cur micelles were combined with an *in situ* gel hydrogel system to form a novel curcumin gel (Cur/HA). The properties of this product were studied for its therapeutic effect on skin trauma models. At present, drug treatment is still the first choice for skin trauma. However, chemical drugs have great irritation to the skin, the clinical use of hormone drugs is still controversial, and there are side effects such as delayed wound healing. In this study, a rat skin defect model was used to creatively compare the hydrogel loaded with Cur and the dexamethasone ointment used in clinic. In this way, two products were compared in order to find the most effective treatment for promoting skin wound healing among the convenient, safe, and low-cost alternatives.

We present the following article in accordance with the ARRIVE reporting checklist (available at https://dx.doi.org/10.21037/atm-21-2872).

Methods

Materials and drugs

Polyethylene glycol (PEG, Mn =4,000), ε-caprolactone (ε-CL) and stannous octanoate [Sn(OCT)2] were purchased from Sigma-Aldrich (St. Louis, MO, USA). Methylene dichloride (CH2Cl2) was purchased from Kelon Chemical Co., Ltd. (Chengdu, China), and the chromatographic levels of methanol and glacial acetic acid were purchased from Sinopill Chemical Reagents Co., Ltd. (Shanghai, China). Curmeric was purchased from Chaoyue Biological Technology Co., Ltd. (Guangzhou, China), anhydrous alcohol was purchased from Kelon Chemical Co., Ltd. (Chengdu, China), and dexamethasone cream was purchased from China Resources Sanjiu Medical & Pharmaceutical Co., Ltd. (Shenzhen, China). The chemicals used in this experiment were all analytical reagent (AR) grade, and were used as is except for PEG.

Animals

Healthy male Sprague Dawley (SD) rats, aged 3–4 weeks

and weighing 130–150 g, were purchased from Chongqing Tengxin Beer Experimental Animal Sales Co., Ltd (Chongqing, China). Animals were kept in cages with free access to food and drinking water and were caged 1 week before the experiment to acclimate to the environment. Experiments were performed under a project license (No. 201903-134) granted by ethics board of the Affiliated Hospital of Southwest Medical University, Luzhou, China, in compliance with national guidelines for the care and use of animals.

Synthesis of the copolymers

In this study, the triblock copolymer PCEC was prepared by ring-opening polymerization according to published protocols (17). First, stannous octanoate Sn(Oct)2 was used as a catalyst to add a certain amount of polyethylene glycol. The amount of ε-CL (the molar ratio of polyethylene glycol to caprolactone was 1:1.1) was calculated and added to the mixture in a 3-necked flask. The reaction was carried out in an oil bath at 130 ℃ for 6 hours under nitrogen gas. After the reaction, the temperature of the reaction system was reduced to room temperature. Dichloromethane was then added until completely dissolved. Excess cold petroleum ether precipitate was added (the volume ratio of petroleum ether to dichloromethane was 4:1). After filtration, the filtrated precipitate was placed in a vacuum drying oven and dried at 40 ℃ for 2 days. The precipitate was removed and sealed for storage.

Preparation and characterization of PCEC/Cur nanmicelles

Cur (4, 8, and 10 mg) and the dry carrier PCEC (96, 92, 90 mg), were mixed and divided into 100 mg aliquots and placed into 3 glass flasks. To each flask of the compound mixture, 10 mL of ethanol was added in order to completely dissolve the compounds. Next, the solvent was completely removed by evaporation (60 ℃, 110 r/min). The evaporate was dissolved in 10 mL of sterile water at 60 ℃, forming a transparent yellow PCEC/Cur nanomicelle solution. The drug-loading (DL) and encapsulation rates (EE) were determined by high performance liquid chromatography (HPLC) [16]. Three groups of 10 mg PCEC/ Cur nanometer micelles with different concentrations were prepared and emulsified with 1 mL of methanol to prepare solutions containing different concentrations of Cur (400, 800, 1,000 μg/L). The solutions were centrifuged in an overspeed refrigerated centrifuge (4 ℃, 12,000 r/min) for 10 minutes. After the centrifugation, 0.5 mL of supernatants was recovered, and 4.5 mL of methanol was added. This stock was then diluted into different concentrations (40, 80, 100 μg/L). The samples were filtered by a 220 nm filter to obtain the suspension for later use. The final Cur content was measured by HPLC. The drug loading and EE were calculated as follows:

$$\text{Drug loading (DL)} = \text{actual amount of curcumin/theoretical amount of curcumin + PCEC polymer amount} \times 100\% \quad [1]$$

$$\text{Encapsulation rate (EE)} = \text{actual amount of curcumin/theoretical amount of curcumin} \times 100\% \quad [2]$$

Cur micelle-HA compound gel preparation

The nanomicelle PCEC/Cur was filtered using a 220-nm filter before freeze-drying at 20 ℃. A freeze-dried yellow solid powder was obtained from 175 mg of sodium hyaluronate dissolved in 5 mL of a saline solution. The 100 mg of freeze-dried nanomicelle Cur was placed on a magnetic stirrer and mixed until homogeneous. A stable hydrogel solution was formed after 24 hours and stored in the dark in a 5-mL syringe until further use.

In vitro release

To investigate the drug release behavior of Cur in free Cur, PCEC/Cur nanomicelles, and Cur/HA, Cur/HA was placed in dialysis bags (the molecular weight retention value was 3.5 kDa). Dialysis bags were immersed in 40 mL of phosphate-buffered saline (PBS; pH=7.4) containing polysorbate-80 (0.5%; w/v) and shaken at 37 ℃ at a rate of 100 r/min. Next, 2 mL of the release medium was extracted at a predetermined time interval (1, 3, 6, 9, 12, 24, 48, 72, 96 and 120 h), and the same volume of fresh preheated release medium was replaced. Samples were collected and analyzed by HPLC at least 3 times for each measurement.

Evaluation of full-thickness skin defect repair in rats

All animals were anesthetized by an intraperitoneal injection of 10% chloral hydrate (3 mL/kg body weight). All Healthy male SD rats are 4–5 weeks old and weigh 140–175 g. The back hair was shaved and disinfected with 75% alcohol. A round full-thickness skin defect wound with a diameter of 23 mm was established. A total of 36 rats with induced skin defect wounds were randomly divided into 4 groups

Table 1 Characterization of the Cur nanomicelles prepared

Sample	Cur:PCEC	DL (%)	EE (%)
1	4:96	3.2±0.5	80.6±0.1
2	8:92	7.2±0.4	90.4±0.1
3	10:90	8.1±1.5	80.6±0.2

Cur, curcumin; PCEC, PCL-b-PEG-b-PCL; DL, drug loading; EE, encapsulation rates.

with 9 rats in each group: (I) blank control group (did not do any treatment, and were only normally fed); (II) blank PCEC/HA gel group; (III) dexamethasone group (positive control group); and (IV) PCEC/Cur nanomicelle combined with HA gel group (treatment group). The corresponding drugs were then applied to the wound surface. The feeding, behavior, and wound changes were observed each day for all rats. At the 0, 7, 14, and 21 days after surgery, the wounds were photographed. IPP 6.0 software was used to measure the initial wound area and the wound area at each time point after surgery at each time point. The following formula was used to calculate the percent reduction of the wound:

$$\text{Wound reduction (\%)} = \frac{WA_0 - WA_t}{WA_0} \times 100\% \quad [3]$$

Histopathologic examination

Four rats in each group were randomly selected and killed at the time points of the first week, the second week and the third week, respectively. The wounds of each rat were fixed with paraformaldehyde, embedded in paraffin, sliced, dewaxed and stained with hematoxylin-eosin-Masson. Three sections were randomly selected from each batch of specimens, and six regions were selected for light microscope photography, histological analysis and collagen formation evaluation.

Immunohistochemical staining

The paraffin sections of the wound tissues were subjected to vascular endothelial growth factor (VEGF)-specific staining, DAB staining, and hematoxylin staining. The positive cells were observed for a brownish-yellow color. For observation under light microscope, 3 sections were randomly selected from each batch of specimens, and six areas were selected for each section to be photographed under the light microscope for evaluation of wound angiogenesis and tissue inflammation.

Statistical analysis

The images were observed and captured under the microscope. SPSS 20.0 software (IBM Corp., Armonk, NY, USA) was used for statistical analysis. The average wound healing rate is expressed as mean ± standard deviation, and the ratio of counting data or composition ratio is used for statistical description. One-way analysis of variance (ANOVA) was used to compare the measurement data between groups, and the least significant difference (LSD) method was used for comparison between groups. The test level was α=0.05.

Results

Preparation and characterization of PCEC/Cur nanomicelles

In this study, PCEC/Cur nanomicelles were prepared by the thin film hydration method. PCEC polymers self-assembled in hot water to form unique "core-shell" structural micelles. In the preparation process of Cur-loaded nan-micelles, the hydrophobic chain segment of Cur was well encapsulated to form the core of the micelles. The hydrophilic PEG block improved the hydrophilic and compliant properties of the polymer and formed the shell of the micelle. In this experiment, 3 nanomicelles were prepared using different concentrations of Cur (4%, 8%, and 10%). The actual drug loading and EE of the PCEC/Cur nanomicelles were measured by HPLC as shown in *Table 1*. Under the condition of constant total weight, the drug loading increased with the increase of the free Cur concentration, but the EE did not significantly increase. The Cur samples with a high loading capacity, high EE, and at a concentration of 8% were selected from the 3 concentration samples for this study.

According to the particle size and potential distribution map shown in *Figure 2A*, it can be seen that the average particle size and average potential of the PCEC/Cur nanomicelles with the drug loading of 8%, are 129 nm and 1.77 mV, respectively. Morphological examination performed with transmission electron microscopy (*Figure 2B*), revealed that most of the micelles were spherical or approximately quasi-spherical, with relatively uniform size and distribution. There was no adhesion or aggregation among particles. *Figure 3* shows the appearance

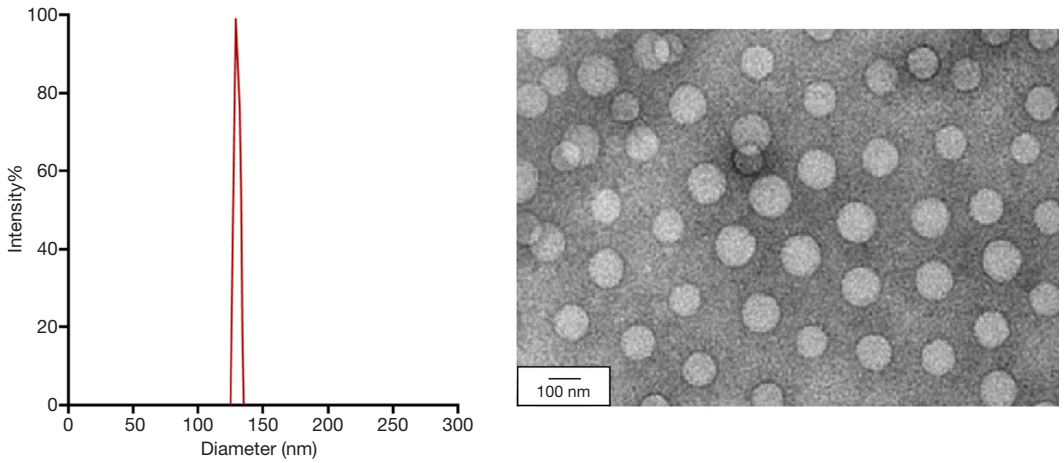

Figure 2 Characterization of particle size and morphology of PCEC/Cur nanomicelles. (A) Particle size distribution of curcumin micelles. (B) Transmission electron microscopy image of curcumin micelles. PECE, PCL-b-PEG-b-PCL; Cur, curcumin.

of the following substances: (I) liquid blank carrier PCEC/HA, (II) blank gel, (III) inverted PCEC/HA blank gel, (IV) free Cur aqueous solution, (V) positive CUR/HA hyaluronic acid gel, (VI) inverted Cur/HA sodium hyaluronate gel. From the figure, we can see that PCEC polymer shows good water solubility in normal saline. In addition, from *Figure 3E,F*, we can see that the prepared Cur nano-micelle-sodium hyaluronate gel is stable and uniform.

In vitro release

Figure 4 shows the effects of hydrogels without Cur (curcumin-free), gels containing PCEC/Cur micelles and curcumin in Cur/HA hydrogels. There was a rapid release of ~80% of the Cur from the PCEC/Cur micelles within 12 h. There was a 72% sustained release of Cur within 12 h from the Cur/HA hydrogels. Cur-free gels showed a quicker release behavior with more than 95% of the Cur released into the medium after 48 h.

Wound morphology

From the initial wounding of a full-thickness skin defect in rats to the end of the experiment, all wounds were free of infection and reached primary healing. No abnormal reactions were observed in the general conditions of the animals, including their diet, mental status, and behavior. The wound healing in rats at different time points is shown in *Figure 5*. During the healing process, there appeared yellow secretions from the wounds in the blank control group. The skin lesions in the blank gel group were moist, bleeding, and ruddy, and appeared dark red on the 14th day. In the dexamethasone group, there was extensive exudation on the wound surface. On the 7th day, there were obvious yellow purulent secretions, which were abundant and thick, and emitted an odor. In the Cur/HA gel group, over the course of the healing process, the wound surface was dry and ruddy, and the granulation tissue was red, tender, and abundant. The epithelial restoration occurred early. The shape of the wound edge was regular, with an obvious contraction. The healing time was also shorter than that in the other 3 groups. On the 14th day after treatment, the average wound healing rate of the blank control group (control group) was 66%±15%. The mean wound healing rate of the blank gel group (blank PCEC/HA gel group) was 71%±14%. The average wound healing rate of the dexamethasone group (positive group) was 88%±2%. The average wound healing rate of the Cur/HA gel group was 96%±3%. The wound healing rate of the Cur/HA gel group was more than 95% on the 14th day of treatment when the wound was nearly fully healed.

Histopathologic examination

The wound healing of the dermal defect was assessed by observing tissue sections. The hematoxylin and eosin (HE) staining of each group at a predetermined time point was conducted for histological analysis. *Figure 6* shows the pathology of the wound tissue after different treatments on day 14. The re-epithelialization of the blank control

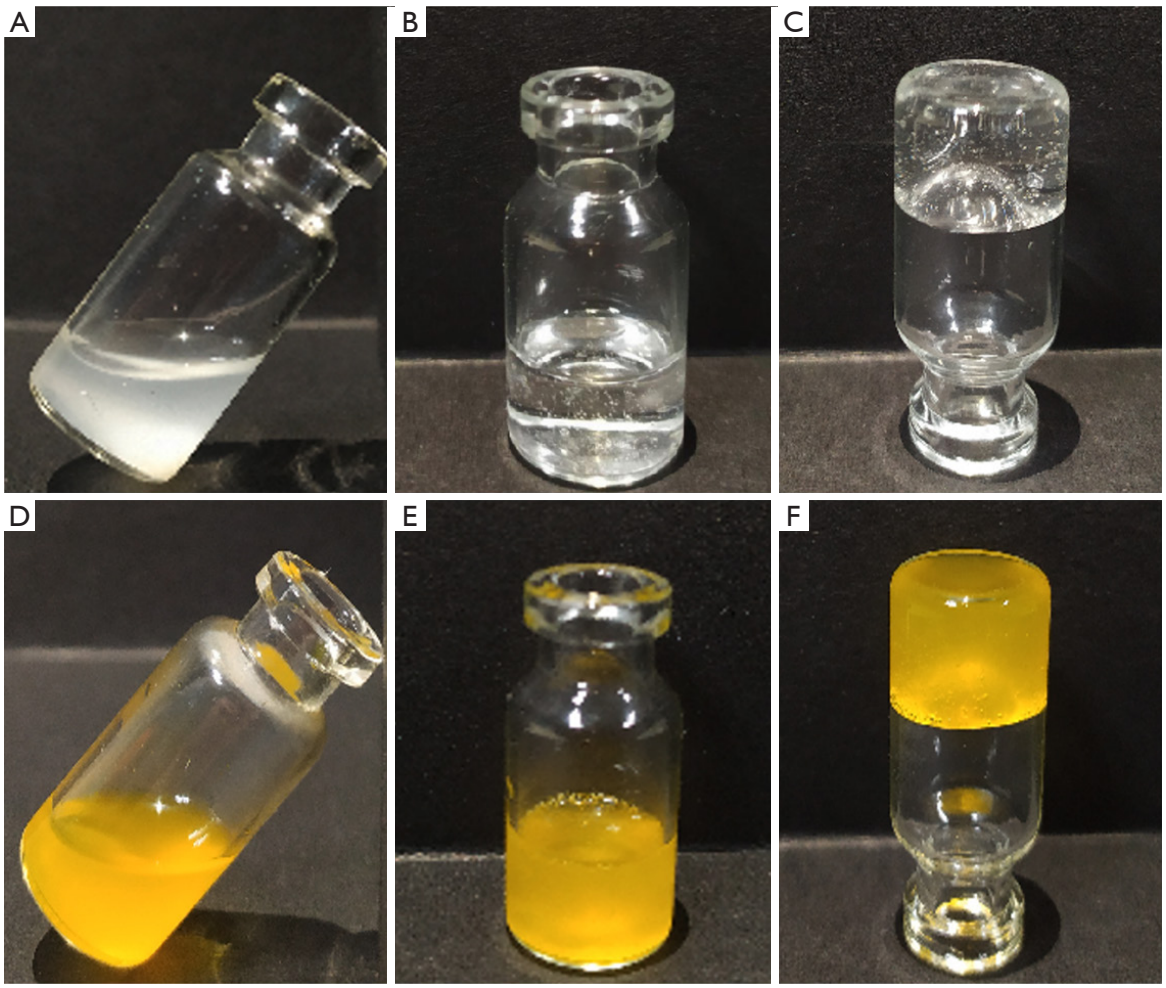

Figure 3 Gel preparations in different states. (A) Liquid blank carrier PCEC/HA, (B) positive PCEC/HA blank gel, (C) inverted PCEC/HA blank gel, (D) free curcumin aqueous solution, (E) orthotopic Cur/HA hyaluronic acid gel, and (F) inverted Cur/HA sodium hyaluronate gel. PECE, PCL-b-PEG-b-PCL; HA, hyaluronic acid.

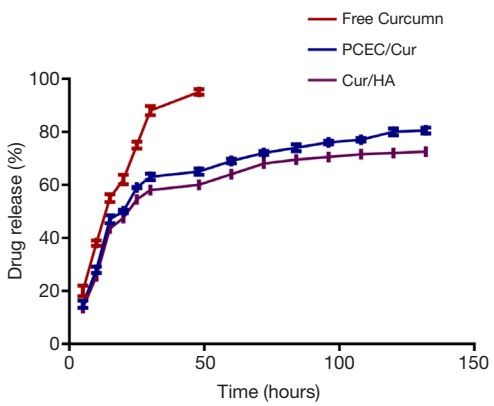

Figure 4 The drug release of curcumin from free curcumin, PCEC/Cur, and Cur/HA. PECE, PCL-b-PEG-b-PCL; Cur, curcumin; HA, hyaluronic acid.

group and blank gel group was not obvious, with infiltration of inflammatory cells and little granulation tissue, and the antibacterial and anti-inflammatory effect was poor (as shown in *Figure 6A*,*B*). In the dexamethasone group, re-epithelialization was not obvious; however, there was obvious ulcer formation with poor healing (*Figure 6A*). A comparison of the 4 groups indicated that the epithelial tissue at the wound edge of the Cur/HA gel group was migrating and close to closure. A complete epithelial structure was observed and re-epithelialization was visible in the wound. In addition, small veins and arterioles were beginning to grow on the wound surface without infiltration of inflammatory cells. Therefore, the antibacterial effect of the Cur/HA gel group was the strongest (*Figure 6D*).

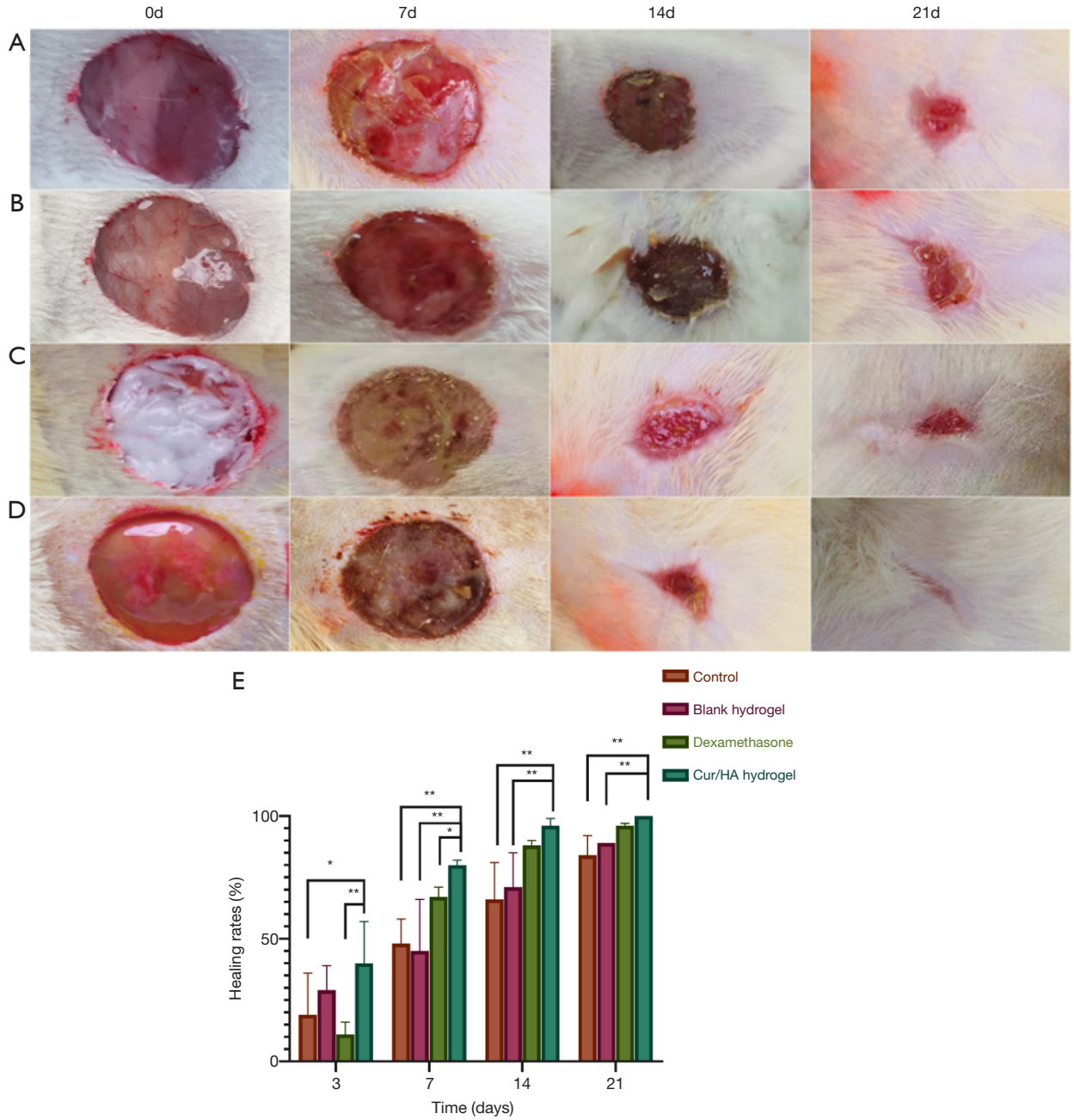

Figure 5 Image of full-thickness skin defect in rats. The wound healing in rats at different time points (A) Evaluation of wound healing after full-thickness skin excision in rats. Group A: blank control; group B: blank gel; group C: dexamethasone; group D: Cur/HA hydrogel. (B) The wound closure rate of the full-thickness dermal wound changed with time. **P<0.01, and *P<0.05. Cur, curcumin; HA, hyaluronic acid.

Figure 7 shows the HE staining of the Cur/HA group at different time periods. On the third day after the modeling of rat skin lesions, re-epithelialization was observed in the HE-stained tissues in the Cur/HA gel group. The damage of the deep subcutaneous tissues was significantly reduced. Inflammatory effects were found in the epidermis and the superficial dermis. On the 7-day, the epidermis was thicker with a stratified structure, and the collagen fibers in the dermis were slightly disordered with no inflammatory cell infiltration. There was abundant capillary growth, more

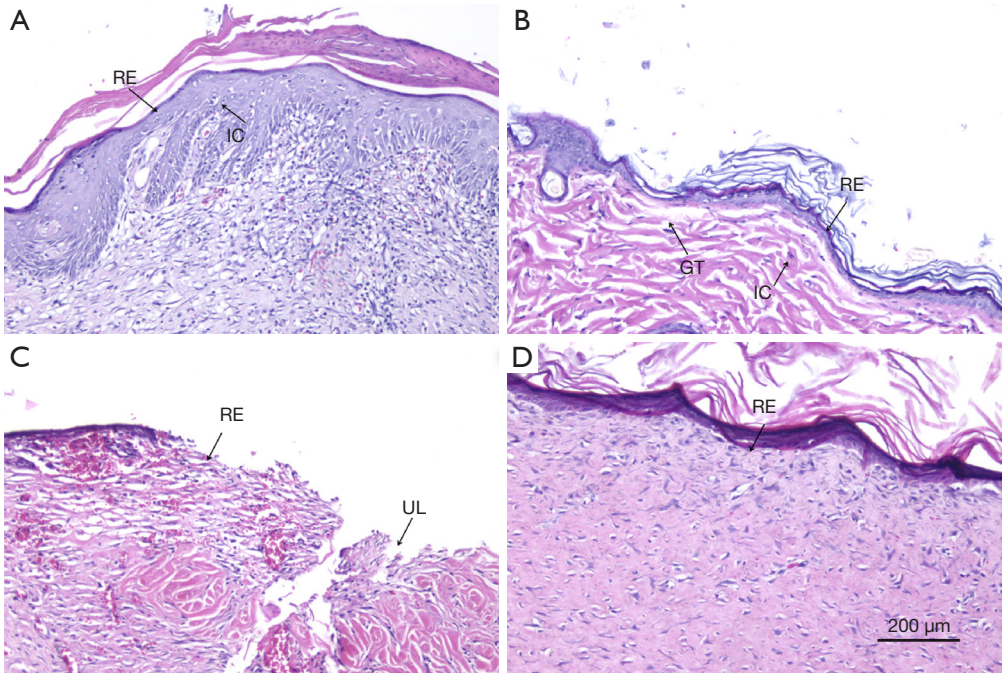

Figure 6 HE staining of skin defects treated with different treatments at 14 days. (A) Blank control group, (B) blank gel group, (C) dexamethasone group, and (D) Cur/HA hydrogel group. HE staining at 100×. HE, hematoxylin-eosin; RE, re-epithelialized; IC, inflammatory cell; GT, granulation tissue; UL, ulcer; BV, blood vessel; Cur, curcumin; HA, hyaluronic acid.

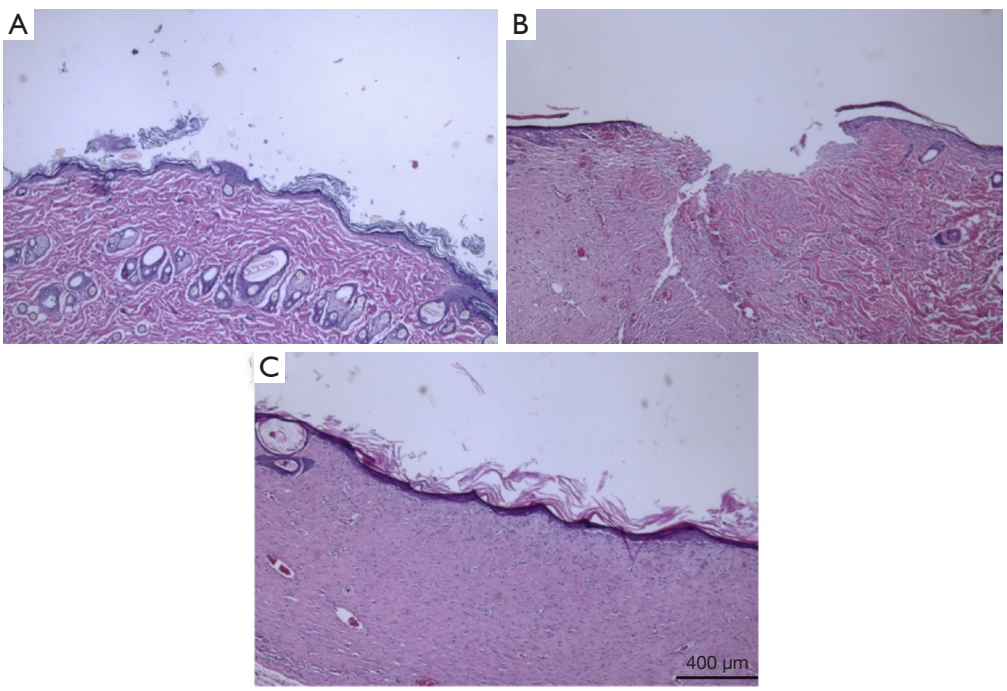

Figure 7 Cur/HA hydrogel group-treated wounds at different time points of HE staining. (A) Day 3, (B) day 7, and (C) day 14. HE staining at 40×. Cur, curcumin; HA, hyaluronic acid; HE, hematoxylin-eosin.

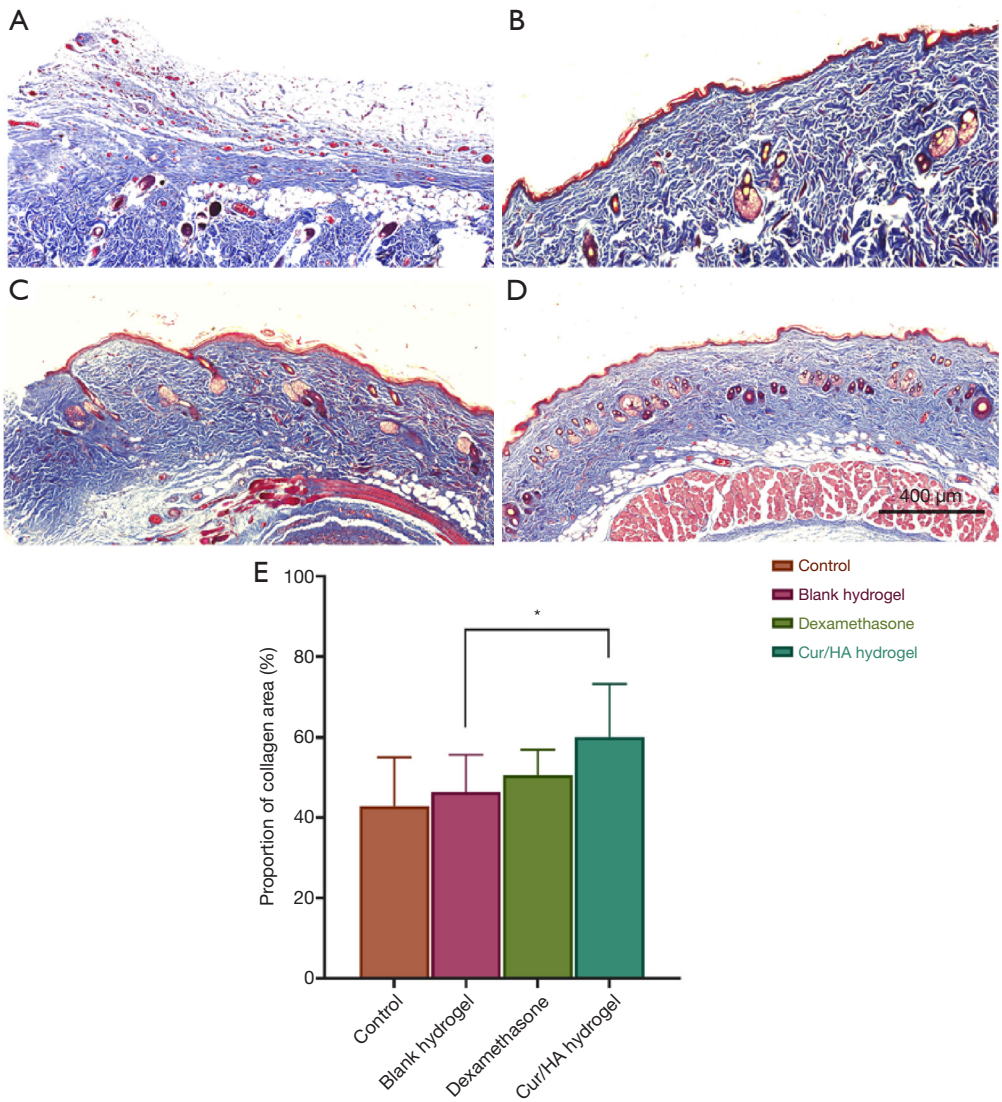

Figure 8 Masson staining of skin defects treated with different treatments at 14 days. (A) Blank control group, (B) blank gel group, (C) dexamethasone group, and (D) Cur/HA hydrogel group. Magnification =100×. (E) The proportion of collagen cells in each group. *P<0.05. Cur, curcumin; HA, hyaluronic acid.

fibroblast proliferation, and granulated tissue growth. On day 14, the wound epithelium was re-epithelialized and granulation tissue was thickened and stratified, the structure was similar to that of the surrounding normal skin, the dermal layer cells gathered obviously and the blood vessels increased. Collagen fibers appeared regularly arranged and no skin appendages were seen. In addition, keratinocytes at the edge of the wound proliferated significantly and began to migrate to the wound center to form an upper belt (i.e., re-epithelialization).

The synthesis and decomposition of collagen fibers is also an important link in the healing of skin defects and wounds, and the results of collagen metabolism directly affect the quality of wound repair. As the main component of ECM, collagen fibers are synthesized by myofibroblasts and fibroblasts. Using the Masson staining method, the contents of the 4 groups of collagen found at the wound site were detected (*Figure 8A*,*B*,*C*,*D*,*E*). Compared with the blank control group, the dexamethasone group, and blank gel group, and the Cur/HA gel showed a larger area following typical collagen arrangement patterns. In addition, the distribution density of the collagen proportion

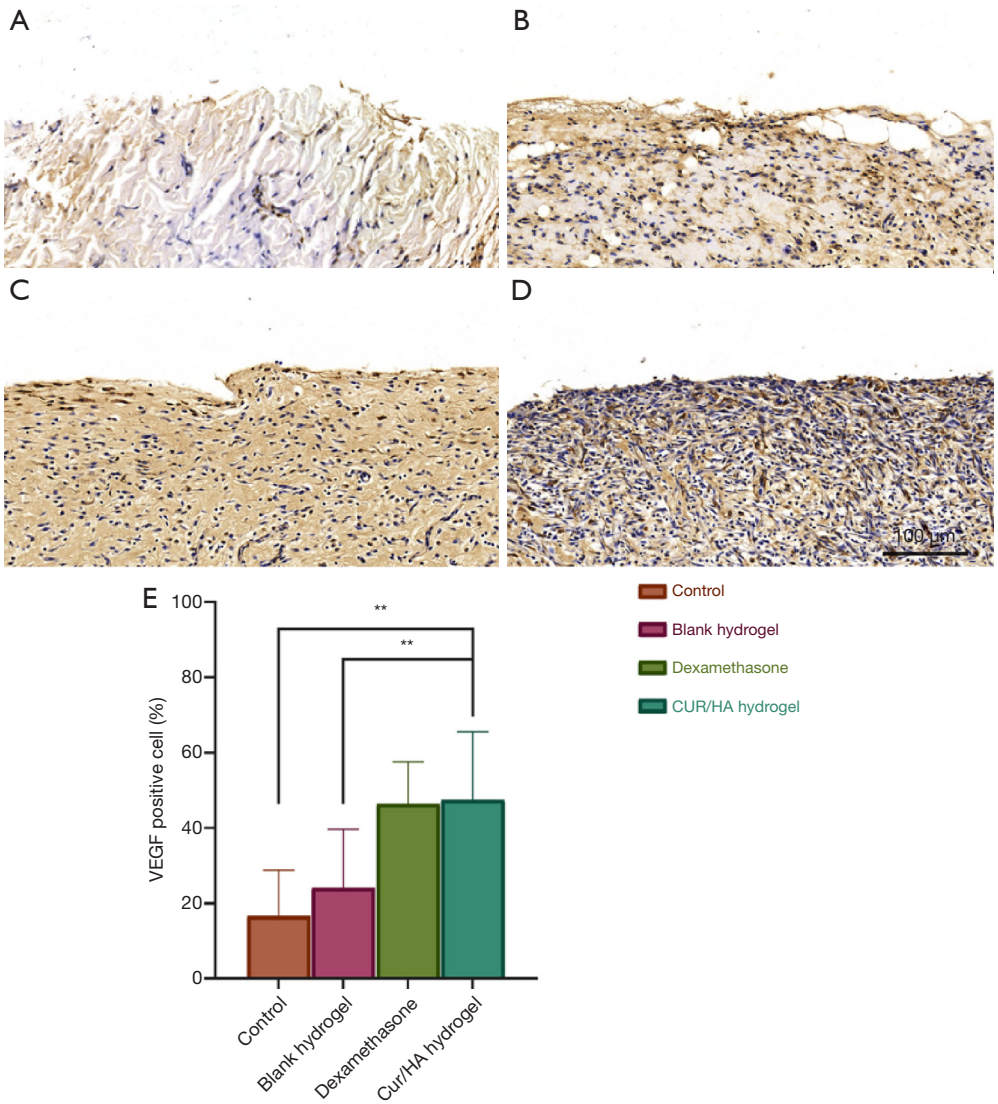

Figure 9 Immunohistochemical staining of VEGF in skin defects of each group. (A) Blank control group, (B) blank gel group, (C) dexamethasone group, and (D) Cur/HA hydrogel group. Magnification =100×. (E) The proportion of positive cells in each group. On the tissue section, all the dark brown was strongly positive, the brown yellow was moderately positive, the light yellow was weakly positive, and the blue nucleus was negative. **P<0.01. Cur, curcumin; HA, hyaluronic acid.

was as high as 60.1%+13.2%. This was significantly higher than that of the control group (42.9%+12.1%), the blank gel group (46.4%+9.2%), and the dexamethasone group (50.5%+6.4%). These results suggest that the Cur/HA gel promotes the synthesis of collagen, which is beneficial to wound healing.

Immunohistochemical observation

New blood vessels are generated at the defect site during the healing process of skin defects and provide oxygen, nutrients, and bioactive substances to the site. This is the basis of tissue repair and an important link in the process of wound healing. Immunohistochemical methods were used to evaluate the effects of different treatments on the angiogenesis of skin defects. As shown in *Figure 9A,B,C,D,E*, the Cur/HA gel group and the dexamethasone group had more VEGF-positive cells (which promote the angiogenesis and healing of the wound surface) compared with the blank gel group and the blank control

group. The proportion of VEGF-positive cells in the blank control group was 16.6%±12.2%, that in the blank gel group was 24.1%±15.6%, that in the dexamethasone group was 46.4%±11.3%, and that in the Cur/HA gel group was 47.54%±18.03% (P<0.001).

Discussion

Skin loss or injury after surgery leaves patients suffering from pain, impaired mobility, excessive exudation, odor of the wound, and limited social interaction (17,18). Therefore, it is important to explore effective drugs and treatments for skin defects. Currently, glucocorticoid drugs such as dexamethasone are widely used. Spreading hormone on the wound surface can reduce the skin damage, but prolonged use can lead to problems such as alterations in local skin pigmentation (19,20). Therefore, the use of such products should be limited. In the present study, curcumin-loaded nanomicelles (PCEC/Cur) were prepared by using the 1-step thin-film hydration method in which Cur was embedded in polymer micelles without any surfactants or additives.

HA has been reported to have positive effects on endothelial cells (21), macrophages (22), keratinocytes (23), and fibroblasts (24). As these cells play an important role in different stages of wound healing, it is important to study the potential effects HA-conjugated Cur may have on these cells in the wound healing process. As previously reported, the coupling of HA with the Cur results in higher stability of HA-Cur in aqueous media than in Cur without HA (25). In order to further understand the wound healing effect of the Cur/HA composite gel in vivo, the product was applied externally to an induced skin wound in a rat model. After the prepared Cur/HA composite gel was applied on the rat wounds, the speed of healing speed was accelerated (*Figure 5A*). In addition, the wound closure rate was significantly higher than that of the control group at 3, 7, and 14 days post surgery. The epidermal re-epithelialization was also accelerated, the inflammatory cells were significantly reduced, and the anti-inflammatory effect was obvious (26). These data indicate an improvement in healing compared to untreated wounds. This result is consistent with previous studies where Cur was found to promote wound healing by increasing collagen deposition (27), fibromy in production, and myofibroblast contraction (28) via its anti-inflammatory and antioxidant activity (26). Compared with the dexamethasone treatment group, the Cur /HA treatment group had good morphology of wound granulation tissue, was rich in collagenous cells, and showed complete re-epithelialization. Likewise, in the Cur/HA treatment group, there were more VEGF-positive cells. This finding was consistent with the results reported by Mani *et al.* (28).

Vascularization is an important link in wound repair, as nascent capillaries provide nutrients for the wound tissue after trauma occurs. In this process, a variety of cells and regulatory factors are involved (29,30). The Cur/HA composite gel promotes the formation of wound capillaries, increases the number of new capillaries, induces the expression of VEGF on the wound, and thus promotes wound healing at the site of injury (31). The improvement of wound healing in the Cur/HA composite gel group may be due to the combined action of HA and Cur on the proliferation and migration of skin cells, as well as dermal collagen deposition (32). Furthermore, the well-formed dermis observed in wounds treated with the Cur/HA composite gel might have arisen due to an increase in HA-induced collagen deposition. Thus, Cur/HA has good biocompatibility and can promote wound healing, making it an excellent candidate for wound dressings and skin tissue engineering.

Conclusions

In this study, a composite gel containing PCEC/Cur and HA was prepared, then used for wound healing evaluation in rats. The results showed that Cur sodium hyaluronate gel could effectively resist infection and inflammation in the process of wound repair, promote local tissue vascularization, and accelerate the healing of wound repair with no obvious adverse reactions *in vivo* or *in vitro*. This novel product has the potential to be a convenient, safe, low-cost alternative for clinical use in promoting wound healing.

Acknowledgments

Funding: This research was funded by the Project of Sichuan Medical Association (no. 2017-Q17080).

Footnote

Reporting Checklist: The authors have completed the ARRIVE reporting checklist. Available at https://dx.doi.org/10.21037/atm-21-2872

Data Sharing Statement: Available at https://dx.doi.org/10.21037/atm-21-2872

Conflicts of Interest: All authors have completed the ICMJE uniform disclosure form (available at Available at https://dx.doi.org/10.21037/atm-21-2872). The authors have no conflicts of interest to declare.

Ethical Statement: The authors are accountable for all aspects of the work in ensuring that questions related to the accuracy or integrity of any part of the work are appropriately investigated and resolved. Experiments were performed under a project license (No. 201903-134) granted by ethics board of the Affiliated Hospital of Southwest Medical University, Luzhou, China, in compliance with national guidelines for the care and use of animals.

References

1. Smith JG. The journal of the American Academy of Dermatology. Int J Dermatol 1979;18:466-7.
2. Akasaka Y, Fujita K, Ishikawa Y, et al. Detection of apoptosis in keloids and a comparative study on apoptosis between keloids, hypertrophic scars, normal healed flat scars, and dermatofibroma. Wound Repair Regen 2001;9:501-6.
3. MacBarb RF, Paschos NK, Abeug R, Makris EA, Hu JC, Athanasiou KA. Passive strain-induced matrix synthesis and organization in shape-specific, cartilaginous neotissues. Tissue Eng Part A 2014;20:3290-302.
4. Stephanopoulos N, Ortony JH, Stupp SI. Self-Assembly for the Synthesis of Functional Biomaterials. Acta Mater 2013;61:912-30.
5. Diekjürgen D, Grainger DW. Polysaccharide matrices used in 3D in vitro cell culture systems. Biomaterials 2017;141:96-115.
6. Li Y, Jiang H, Zheng W, et al. Bacterial cellulose-hyaluronan nanocomposite biomaterials as wound dressings for severe skin injury repair. J Mater Chem B 2015;3:3498-507.
7. Deng Z, Jin J, Wang S, et al. Narrative review of the choices of stem cell sources and hydrogels for cartilage tissue engineering. Ann Transl Med 2020;8:1598.
8. Anand K, Ray S, Rahman M, et al. Nano-emulgel: Emerging as a Smarter Topical Lipidic Emulsion-based Nanocarrier for Skin Healthcare Applications. Recent Pat Antiinfect Drug Discov 2019;14:16-35.
9. Dai T, Wang C, Wang Y, Xu W, Hu J, Cheng Y. A Nanocomposite Hydrogel with Potent and Broad-Spectrum Antibacterial Activity. ACS Appl Mater Interfaces 2018;10:15163-73.
10. Dong R, Zhao X, Guo B, et al. Self-Healing Conductive Injectable Hydrogels with Antibacterial Activity as Cell Delivery Carrier for Cardiac Cell Therapy. ACS Appl Mater Interfaces 2016;8:17138-50.
11. Zhang T, Liu F, Tian W. Advance of new dressings for promoting skin wound healing. Sheng Wu Yi Xue Gong Cheng Xue Za Zhi 2019;36:1055-9.
12. Li S, Dong S, Xu W, et al. Antibacterial Hydrogels. Adv Sci (Weinh) 2018;5:1700527.
13. Yao M, Yang L, Wang J, et al. Neurological recovery and antioxidant effects of curcumin for spinal cord injury in the rat: a network meta-analysis and systematic review. J Neurotrauma 2015;32:381-91.
14. Aggarwal BB, Gupta SC, Sung B. Curcumin: an orally bioavailable blocker of TNF and other pro-inflammatory biomarkers. Br J Pharmacol 2013;169:1672-92.
15. Panahi Y, Fazlolahzadeh O, Atkin SL, et al. Evidence of curcumin and curcumin analogue effects in skin diseases: A narrative review. J Cell Physiol 2019;234:1165-78.
16. Kharat M, Du Z, Zhang G, et al. Physical and Chemical Stability of Curcumin in Aqueous Solutions and Emulsions: Impact of pH, Temperature, and Molecular Environment. J Agric Food Chem 2017;65:1525-32.
17. Jia W, Gu Y, Gou M, et al. Preparation of biodegradable polycaprolactone/poly (ethylene glycol)/polycaprolactone (PCEC) nanoparticles. Drug Deliv 2008;15:409-16.
18. Ramshankar YV, Suresh S. A Sensitive Reversed Phase HPLC Method for the Determination of Curcumin. Pharmacogn Mag 2009;4:71-4.
19. Rein DT, Kurbacher CM, Breidenbach M, et al. Weekly carboplatin and docetaxel for locally advanced primary and recurrent cervical cancer: a phase I study. Gynecol Oncol 2002;87:98-103.
20. da Silva JM, Conegundes JLM, Pinto NCC, et al. Comparative analysis of Lacistema pubescens and dexamethasone on topical treatment of skin inflammation in a chronic disease model and side effects. J Pharm

Pharmacol 2018;70:576-82.
21. Zhang M, Gao J, Zhao X, et al. p38α in macrophages aggravates arterial endothelium injury by releasing IL-6 through phosphorylating megakaryocytic leukemia 1. Redox Biol 2021;38:101775.
22. Lee M, Wang C, Jin SW, et al. Expression of human inducible nitric oxide synthase in response to cytokines is regulated by hypoxia-inducible factor-1. Free Radic Biol Med 2019;130:278-87.
23. Bourguignon LY, Wong G, Xia W, et al. Selective matrix (hyaluronan) interaction with CD44 and RhoGTPase signaling promotes keratinocyte functions and overcomes age-related epidermal dysfunction. J Dermatol Sci 2013;72:32-44.
24. David-Raoudi M, Tranchepain F, Deschrevel B, et al. Differential effects of hyaluronan and its fragments on fibroblasts: relation to wound healing. Wound Repair Regen 2008;16:274-87.
25. Dey S, Sreenivasan K. Conjugation of curcumin onto alginate enhances aqueous solubility and stability of curcumin. Carbohydr Polym 2014;99:499-507.
26. Yang BY, Hu CH, Huang WC, et al. Effects of Bilayer Nanofibrous Scaffolds Containing Curcumin/Lithospermi Radix Extract on Wound Healing in Streptozotocin-Induced Diabetic Rats. Polymers (Basel) 2019;11:1745.
27. Guo C, Li M, Qi X, et al. Intranasal delivery of nanomicelle curcumin promotes corneal epithelial wound healing in streptozotocin-induced diabetic mice. Sci Rep 2016;6:29753.
28. Mani H, Sidhu GS, Kumari R, et al. Curcumin differentially regulates TGF-beta1, its receptors and nitric oxide synthase during impaired wound healing. Biofactors 2002;16:29-43.
29. Kant V, Gopal A, Pathak NN, et al. Antioxidant and anti-inflammatory potential of curcumin accelerated the cutaneous wound healing in streptozotocin-induced diabetic rats. Int Immunopharmacol 2014;20:322-30.
30. Gordon S, Martinez FO. Alternative activation of macrophages: mechanism and functions. Immunity 2010;32:593-604.
31. Suarato G, Bertorelli R, Athanassiou A. Borrowing From Nature: Biopolymers and Biocomposites as Smart Wound Care Materials. Front Bioeng Biotechnol 2018;6:137.
32. Duan Y, Li K, Wang H, et al. Preparation and evaluation of curcumin grafted hyaluronic acid modified pullulan polymers as a functional wound dressing material. Carbohydr Polym 2020;238:116195.

(English Language Editor: J. Gray)

Cite this article as: Zhou P, Zhou H, Shu J, Fu S, Yang Z. Skin wound healing promoted by novel curcumin-loaded micelle hydrogel. Ann Transl Med 2021;9(14):1152. doi: 10.21037/atm-21-2872

